

# ReinhardGAN Hybrid Strategic Light Optimization for Normalization of H E Stained Colorectal Cancer

Shubhajit Panda<sup>1</sup>, Mahesh Jangid<sup>2,\*</sup>, Ashish Jain<sup>3</sup>

<sup>1</sup>Department of Computer Science and Engineering, Manipal University Jaipur, Jaipur, Rajasthan, India

<sup>2</sup>Department of Computer Science and Engineering, Manipal University Jaipur, Jaipur, Rajasthan, India

<sup>3</sup>Department of Computer Science and Engineering, Institute of Engineering and Technology, JK Lakshmi Pat University, Jaipur, Rajasthan, India

## Abstract

Stain normalization is a crucial pre-processing process for the accurate interpretation of Haematoxylin and Eosin (H&E) stained histopathology images based on colorectal cancer. Effective normalization improves classification accuracy by reducing computational complexity, addressing inter-variability in background colors across a dataset, and minimizing data loss. This paper proposes a novel approach that combines Reinhard normalization with a Generative Adversarial Network (ReinhardGAN) to enhance image color properties, such as consistency, contrast, and luminance. To further optimize the normalization process, a Hybrid Strategic Light Optimization (HSLO) algorithm is introduced, minimizing the loss and computational cost during the H&E-stained image normalization. The experimental results demonstrate that the proposed ReinhardGAN-HSLO provided outstanding performance over conventional color normalization methods in terms of colour consistency and normalization as indicated by qualitative and quantitative assessments

Received on 01 October 2025; accepted on 12 May 2026; published on 18 May 2026

**Keywords:** Arithmetic Optimization Algorithm, Hematoxylin and Eosin, Normalization, Reinhard Stain Normalization, War Strategy Optimization

Copyright © 2026 Shubhajit Panda *et al.*, licensed to EAI. This is an open access article distributed under the terms of the [CC BY-NC-SA 4.0](#), which permits copying, redistributing, remixing, transformation, and building upon the material in any medium so long as the original work is properly cited.

doi:10.4108/eetpht.11.10445

## 1. Introduction

Histopathology, which depends on tissue-level investigation, that provides that are suspected of being diseased, especially malignancies for accurate clinical diagnosis and treatment decisions [1]. This is different from radiology, which provides macroscopic imaging. A pathologist looks at stained tissue samples to find structural and morphological patterns in order to confirm a cancer diagnosis. However, the visual quality of histopathology images is frequently impacted by changes in staining, variations in scanners, and manual tissue sectioning, which results in inconsistent colouration among samples [2]. If there is any variation in the staining process, whether it is caused by the concentration of the reagent or inconsistencies in the procedure, it could have a major effect on the dependability of computer-aided histopathology analysis.

The Hematoxylin & Eosin (H&E) staining method is the most commonly utilised. In this procedure, hematoxylin stains the nuclei purple, while eosin stains the cytoplasm pink [3]. H&E staining is essential for diagnosing colorectal cancer (CRC). To overcome these challenges, a number of stain normalization techniques have been proposed that standardize colour differences across histopathological images [4]. Grey-level transformations, red-blue ratio analysis, and Reinhard normalization are some of the traditional methods that can be used to align images to a target colour space. Although these procedures improve uniformity, they frequently do not maintain important tissue features, which results in the loss of information [5].

Early detection of CRC greatly increases the chances of survival, but the presence of stain variations makes automated analysis and AI-based classification more difficult [6]. In addition, AI-based models that are

\*Corresponding author. Email: [mahesh.jangid@jaipur.manipal.edu](mailto:mahesh.jangid@jaipur.manipal.edu)

trained on unnormalized experience reduced generalization as a result of inconsistencies in staining. The absence of homogeneous staining techniques is a significant restriction in digital pathology, because it leads to differences in how colours are seen [7]. Due to irregularities in the concentration of the reagents, the same tissue sample may appear in different hues of blue, pink, or red. This might create difficulties when it comes to nucleus segmentation and classification algorithms. Although colour normalization has been demonstrated to improve the differentiation of image components (such as nuclei, cytoplasm, and background), there is a lack of quantitative research in previous publications about its effect on deep learning models [8].

This paper presents an Optimization-Driven Hybrid Deep Learning Framework that combines Reinhard stain normalization with deep learning techniques in order to overcome these issues. A new hybrid optimization based on Hybrid Strategic Light Optimization (HSLO) algorithm is developed to improve colour consistency while maintaining structural integrity. The suggested method decreases the amount of information that is lost, enhances the brightness of the background, and reduces the complexity of the calculations, which makes CRC detection more precise and effective. This study intends to establish a new standard for stain normalisation in digital pathology that is both robust and reproducible by harmonising Reinhard normalization with AI-driven refining.

### 1.1. Problem Statement

H and E stained colorectal cancer histopathology images stained with HE and E exhibit considerable color variability due to variations in staining procedures, scanner characteristics and tissue properties. This inconsistency presents challenges in the accurate interpretation and classification of cancerous tissues, as it hampers the uniformity required for reliable image analysis. While existing color normalization methods attempt to address these challenges, they often fall short of fully compensating for discrepancies in colour intensity, contrast, and luminance, which ultimately leads to suboptimal classification performance and increased computational complexity. Hence, a more advanced and robust color normalization technique is needed that not only improves the consistency and uniformity of H & E-stained images but also preserves critical histological features, thereby allowing more accurate and efficient cancer classification.

### 1.2. Contribution

- Reinhard Normalization with Generative Adversarial Networks (ReinhardGAN) method aligns the colour distribution between images, transforming them from the RGB colour space to the

Lab colour space and subsequently back to RGB after normalization.

- The GAN framework is employed to refine the image, improving consistency, contrast, and luminance while maintaining critical histological features.
- A Hybrid Strategic Light Optimization (HSLO) algorithm combines a Light Spectrum Optimizer (LSO) and War Strategy Optimization (WSO) to ensure that both the generator (in the deep learning model) and the discriminator (in the adversarial network) are trained in loss. The algorithm optimises their respective losses to guarantee high-quality colour normalization while preserving structural integrity.
- The proposed method is rigorously evaluated using both qualitative and quantitative metrics. Local quality metrics assess the normalization process's performance, demonstrating that the method significantly outperforms existing benchmark techniques in terms of colour consistency, contrast, and luminance.

## 2. Literature review

Stain normalization is a critical preprocessing step in histopathological image analysis, aimed at reducing color variability caused by differences in staining protocols, scanners, and tissue preparation. Existing approaches can be broadly categorized into statistical color transfer methods, enhanced rule-based techniques, and learning-based models.

Early methods focused on statistical color normalization, where image distributions are aligned in a perceptually uniform color space. The approach proposed by Reinhard et al. [9] remains one of the most widely adopted techniques, using mean and standard deviation matching in the Lab color space. Although computationally efficient, such methods are sensitive to stain variability and often fail to preserve fine structural details, limiting their robustness in heterogeneous datasets.

To overcome these limitations, several studies introduced modifications to the classical Reinhard framework. The improved variants [10], [11] focus on better luminance handling and optimized color vector selection, leading to improved segmentation performance and reduced processing time. Similarly, extensions based on fuzzy logic [13] aim to improve global color consistency and contrast. Despite these advancements, these methods remain largely deterministic and lack adaptability to complex, non-linear staining variations.

Another research direction integrates preprocessing strategies with normalization techniques. Methods

combining Reinhard normalization with filtering, histogram equalization, and gamma correction [14] demonstrate improvements in image quality metrics such as SSIM and MSE. However, these approaches introduce additional parameter dependencies and do not explicitly address the computational cost or optimization of normalization loss, which are critical for large-scale applications.

With the advancement of deep learning, learning-based stain normalization approaches have gained prominence. Convolutional Neural Network (CNN)-based frameworks [15] and transfer learning approaches [16] show that normalization significantly improves classification performance. However, in most cases, normalization is treated as a separate preprocessing step rather than being integrated into the learning pipeline, limiting overall optimization.

More recently, Generative Adversarial Networks (GANs) have been employed to model complex stain distributions. Approaches such as MultiStain-CycleGAN [17] enable multi-domain normalization without requiring retraining for each stain variation, while GAN-based extensions of Reinhard normalization [18] improve structural preservation and classification accuracy. Despite their effectiveness, these models often involve high computational complexity, training instability, and limited analysis of optimization efficiency.

Overall, the progression of stain normalization techniques demonstrates a transition from statistical methods to data-driven learning approaches. However, several challenges remain unresolved. Traditional methods lack adaptability to diverse staining conditions, whereas deep learning approaches incur significant computational cost and often do not jointly optimize color consistency, luminance, and structural preservation. Furthermore, limited attention has been given to efficient loss optimization strategies for stabilizing adversarial training.

To address these limitations, the proposed work introduces a hybrid framework that integrates Reinhard normalization with a GAN-based refinement process, optimized using a Hybrid Strategic Light Optimization (HSLO) algorithm. Unlike existing approaches, the proposed method simultaneously focuses on improving color consistency, preserving structural integrity, and minimizing computational and optimization loss. Table 1 provides a comparative summary of existing methods and supports the discussion presented in this section.

---

#### Algorithm 1 Image Normalization using Reinhard Standardization

---

**Require:** Source image  $S$ , Target image  $T$  (RGB format)

**Ensure:** Normalized image  $N$  (RGB format)

- 1: Read the Source image  $S$ , Target image  $T$
  - 2: Convert RGB to  $l\alpha\beta$  colour space:
  - 3:   Convert RGB image to XYZ color space
  - 4:   Convert the XYZ image to LMS cone space
  - 5:   Apply logarithmic transformation to remove skew
  - 6:   Transform the LMS space to  $l\alpha\beta$  space
  - 7: Initialize the variable:
  - 8:   Set the channel index  $i = 0$
  - 9:   Set the number of channels  $c = 3$  (for  $l\alpha\beta$  components)
  - 10: Apply channel-wise transformation:
  - 11: **for** each channel  $i$  in  $\{l, \alpha, \beta\}$  **do**
  - 12:   Compute the transformed pixel values using the Reinhard standardization formula:
  - 13:      $\lambda = \text{mean}(\lambda_T) + (\lambda_S - \text{mean}(\lambda_S)) \times \frac{\text{std}(\lambda_T)}{\text{std}(\lambda_S)}$
  - 14:      $\alpha = \text{mean}(\alpha_T) + (\alpha_S - \text{mean}(\alpha_S)) \times \frac{\text{std}(\alpha_T)}{\text{std}(\alpha_S)}$
  - 15:      $\beta = \text{mean}(\beta_T) + (\beta_S - \text{mean}(\beta_S)) \times \frac{\text{std}(\beta_T)}{\text{std}(\beta_S)}$
  - 16: **end for**
  - 17: Convert the transformed  $l\alpha\beta$  image into an RGB image.
  - 18: **Return** Normalized image  $N$  (RGB format)
- 

### 3. Proposed Methodology

To ensure reliable and consistent interpretation of histopathological images, it is essential to standardize image color properties. In this context, Reinhard normalization plays a fundamental role as an effective color normalization technique. In the preliminary phase, Reinhard normalization [19] is applied to the input images to reduce inter-image color variability. This method operates by transforming the image from the RGB color space to the perceptually uniform Lab color space, where  $L$  represents lightness,  $a$  corresponds to the green–red axis, and  $\beta$  denotes the blue–yellow axis. The normalization process aligns the color distribution of images by matching the channel-wise mean and standard deviation of the source image to those of a target reference image.

Subsequently, the normalized image is converted back to the RGB color space to obtain the final output. This transformation ensures that images acquired under varying staining conditions and scanning devices are standardized to a consistent color representation. The Lab color space is particularly suitable for H&E-stained histopathological images, as it facilitates the separation of hematoxylin (blue–purple) and eosin (pink–red) stain components through independent chromatic channels. As a result, the method effectively

**Table 1.** Comparison of Stain Normalization Methods in Histopathology Images

Author	Method	Aim	Advantage	Disadvantage
Reinhard, E., et al. (2001)	Colour transformation-based method	Transfer colour characteristics from one image to another	Effective colour correction	Loss, Complex, Variation in stain intensity
Roy, S. et al. (2021)	Modified Reinhard algorithm	Colour normalization of colorectal cancer histopathology images	Handled background luminance	Computational complexity, Not support to DL
Piórkowski, A., et al. (2019)	Colour normalization approach	To perform nuclei segmentation in H&E-stained tissue	Promote contrast in lower intensity region	Computational complexity
Roy, et al. (2019)	Fuzzy-based modified Reinhard colour normalization	Colour normalization method for H&E images	Better correlation coefficient, global mean colour consistency, and image contrast	Computational complexity, Not considered luminance
Rabeya, R. A., et al. (2024)	Reinhard approach with bilateral filter, CLAHE, and gamma correction	Conventional stain normalization	Handled effects of pixel distribution, median value, and relative variability	High cost, Loss not considered
Yengec-Tasdemir, et al. (2023)	Convolutional Neural Network	Stain normalization techniques	Accuracy 95%	Loss and luminance not considered
Lee, J., et al. (2022)	Reinhard with machine learning	Identifying important visual features	Imbalance data handled	High computational cost, Loss
Hetz, et al. (2024)	MultiStain-CycleGAN	Stain normalization, multi-domain approach	Achieve better structural similarity index	High complexity
Alhassan, A. M. (2024)	Reinhard-GAN-IGTO	Improve Reinhard stain normalization using GAN	Efficient feature extraction, Minimum loss, High accuracy 98%	High computational complexity, Luminance not considered

reduces color variability, corrects background inconsistencies, and enhances visual uniformity, thereby improving the reliability of downstream analysis tasks.

Following the normalization stage, a deep learning-based refinement process is employed to further enhance image quality. Specifically, a Generative Adversarial Network (GAN) [20] is utilized to improve color consistency, contrast, and luminance across the dataset. The GAN framework is designed to preserve critical histological structures while adapting the color distribution to match high-quality reference images. To optimize the overall process, a Hybrid Strategic Light Optimization (HSLO) algorithm is integrated, enabling coordinated training of the generator and discriminator networks through effective minimization of their respective loss functions. This joint optimization ensures improved normalization performance while

maintaining structural integrity and reducing computational inefficiencies [22]. The overall architecture of the proposed model is illustrated in Figure 1.

### 3.1. Dataset

NCT-CRC-HE-100K is a large-scale dataset specifically designed for colorectal cancer (CRC) research, and it consists of 100,000 H&E-stained histopathological images. These images are part of the National Centre for Tumour Diseases (NCT) dataset focused on CRC. The NCT-CRC-HE-100K dataset captures this variability, making it ideal for training models (including GANs) that can learn to normalize colour and compensate for staining differences. According to that, if the dataset contains whole-slide images (WSIs), you will first need to segment or crop these into smaller patches that are suitable for analysis (e.g., 256x256 pixels).

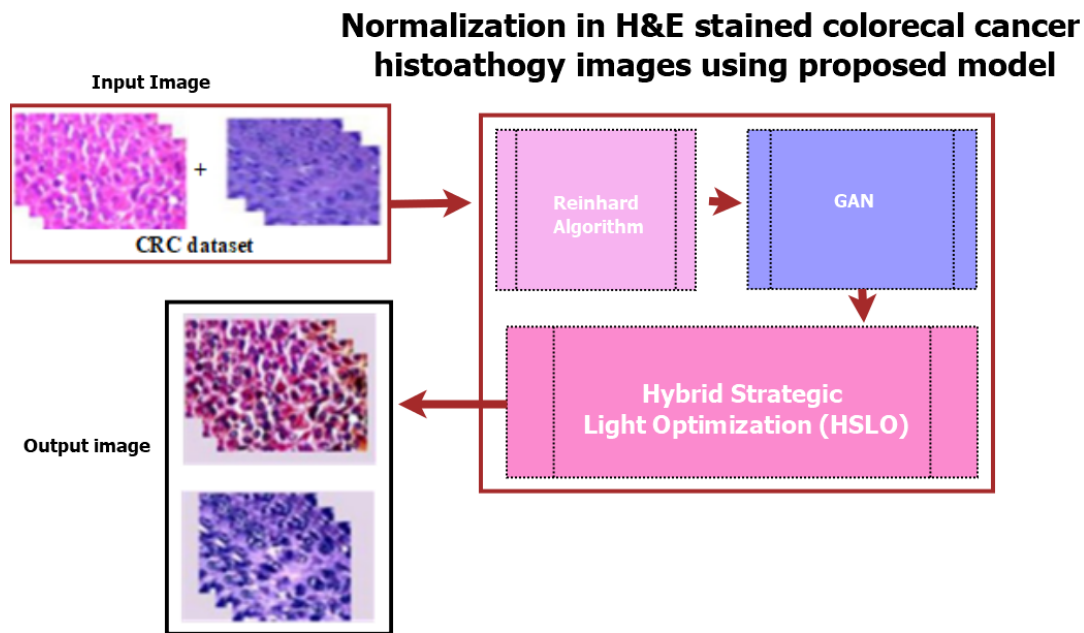


Figure 1. A proposed convolutional neural network (CNN) architecture for colon cancer detection

Laplacian variance filter is used to remove the blurry, low-resolution image. Thus, it ensures that the high-resolution, meaningful images are retained for tasks like colour normalization and stain analysis while removing poor-quality or distorted images.

### 3.2. Reinhard stain normalisation

Reinhard stain normalisation aims to standardise the colour distribution of an image to match a reference image. This ensures that the Hematoxylin (blue/purple) and Eosin (red/pink) stains are consistently represented across different images, even if they were stained or scanned under different conditions. For CRC diagnosis, this consistency helps ensure that the model focuses on relevant features (like tumour regions, glands, or nuclei) and not on artificial differences caused by the staining process. This method offers a refined approach to color normalization by seamlessly adjusting the color distribution of an under-stained or over-stained image to match that of a well-stained target image. Utilizing a linear transformation in the color space, it precisely aligns the mean and standard deviation of each color channel, ensuring a harmonious color balance. Unlike conventional techniques, this approach not only transfers the target image's mean color but also preserves the natural intensity variations of the source image, maintaining its structural integrity. The result is a processed image that mirrors the target in color consistency while retaining the original contrast and details. This makes it a powerful tool for histopathological image analysis, where accurate color

representation and consistency are crucial for reliable interpretation and diagnosis.

### 3.3. ReinhardGAN

The limitations of the Reinhard stain normalization method are effectively addressed by ReinhardGAN, a deep learning-based approach that enhances colour normalization while preserving structural integrity and background illumination. Unlike Reinhard's method, which relies on a fixed reference image, ReinhardGAN dynamically learns stain distribution patterns and illumination variations from a diverse dataset, ensuring a better adaptation to stain variability and lighting inconsistencies across different histopathology images. By leveraging a Generative Adversarial Network (GAN), ReinhardGAN mitigates overcorrection, prevents distortion in stain intensity, and maintains natural color variations while ensuring consistency across samples. Additionally, its ability to learn spatial and illumination features enables better tissue structure preservation, preventing the loss of morphological details crucial for diagnosis and segmentation tasks. Unlike traditional methods, ReinhardGAN effectively normalizes background illumination, reducing the impact of scanner-dependent lighting variations and ensuring better contrast balance in stained images. Overall, ReinhardGAN outperforms traditional normalization techniques by offering a data-driven, adaptive approach to stain normalization and illumination correction, making it more robust, generalizable, and clinically reliable for digital pathology applications. The resulting image serves as

an initially normalized image but may still contain imperfections due to reference-image dependency.

A Generative Adversarial Network (GAN) is used to further refine stain normalization by learning an optimal stain distribution from a diverse set of histopathology images shown in Figure 2. To enhance feature extraction, the architecture incorporates a multiscale extraction module that utilizes  $1 \times 1$ ,  $3 \times 3$ , and  $5 \times 5$  convolution kernels. The  $1 \times 1$  convolution helps in dimensionality reduction and feature fusion, the  $3 \times 3$  convolution captures local spatial patterns, and the  $5 \times 5$  convolution extracts broader contextual information. This combination enables efficient feature representation across multiple scales.

The model extracts deep features using  $5 \times 5$  and  $7 \times 7$  convolutions, fusing them into synthetic representations. Three  $1 \times 1$  convolutions reduce dimensions from 128 to 64, followed by attention refinement. A final  $1 \times 1$  convolution compresses features to a single dimension, producing a clear luminance image. The discriminator evaluates the quality of the generated image by comparing it against real H and E images, guiding the generator to produce realistic stain-normalized outputs.

The discriminator is a key part of the GAN architecture that distinguishes genuine and synthetic images. It uses an adaptive pooling layer and six convolutional layers (CLs) to collect and refine characteristics to verify image authenticity. The first convolutional layer raises input dimensionality from 1 to 64, allowing low-level feature extraction. The second layer adds 128 dimensions to the model, allowing it to capture more intricate spatial patterns. The third convolutional layer captures greater visual information by increasing dimensions to 256 as the network deepens, improving feature expressiveness. This is followed by the fourth layer, which expands dimensions to 512 to help the discriminator understand the image's structural and textural information. The fifth convolutional layer keeps dimensionality at 512, preserving the retrieved features' high-level representational capacity. The sixth layer shrinks the dimensions to 1 to create the output layer. A sigmoid activation function is used at this stage to provide an output in the range  $[0,1]$ , where values closer to 1 indicate a real image and those near 0 are a fake image. Binary classification gives input for generator improvement, making it vital for GAN training.

During its update phase, the discriminator aims to distinguish actual and fraudulent photos as well as possible. In contrast, the generator's update phase aims to create synthetic images that mislead the discriminator and look authentic. Both networks improve as adversarial training progresses—the generator increases its synthetic picture quality while the discriminator evaluates more realistic images. The generator has learned the data distribution when the discriminator can no longer

distinguish real from fake images, reaching a Nash equilibrium. In this equilibrium, the GAN generates realistic stain-normalized images at its best.

In adversarial learning, the generator and discriminator optimize their performance through adversarial loss, comprising generator and discriminator loss. The loss of the discriminator is crucial to distinguish real from synthetic data, enhancing the realism of the image. The equation for discriminator loss in GANs is shown below.

$$\max_{D_L} L(D_L) = \mathbb{E}_{y_1 \sim q(y_1)} [\log D_L(y_1)] + \mathbb{E}_{y_2 \sim q(y_2)} [\log D_L(y_2)] + \mathbb{E}_{x \sim q(x)} [\log (1 - D_L(G(x)))] \quad (1)$$

where  $L(G_L)$  denotes the minimum loss function of the generator.

**Generator Loss** During the generator's update phase, the discriminator remains inactive, allowing the generator to focus solely on refining its ability to produce realistic outputs. This simplifies the generator loss function by eliminating discriminator-related terms, ensuring that the update process is driven purely by the generator's performance in fooling the discriminator. By doing so, the generator can optimize its parameters without interference, learning to generate images that closely resemble real data. This strategic isolation enhances the stability of adversarial training and promotes more efficient convergence, ultimately improving the quality of synthesized images [23].

**Colour consistency loss** The purpose of Color Consistency Loss [24] is to penalise differences in the colour distributions (particularly in the chromatic components) between the generated image and the target image after normalization. The goal is to align the color characteristics of the generated image with the reference target image. Color consistency loss is shown in Equation 3,

$$LOSS_{color} = \|G(x) - T\|_2 \quad (2)$$

Where  $G(x)$  denotes the generated image from the GAN model, given input  $x$ , and  $T$  indicates the target reference images. The norm  $\|\cdot\|_2$  represents the squared L2 norm (Euclidean distance), which measures the difference between the means and standard deviations of the color distributions.

**Illumination Loss** Illumination loss often refers to a component of the overall loss function designed to specifically penalize the generator for not accurately capturing the illumination aspects of a real image, typically achieved by comparing the generated image's luminance distribution with that of the ground truth image; the formula can be expressed as [25].

$$LOSS_{illum} = \|I(G(x)) - I(T)\| \quad (3)$$

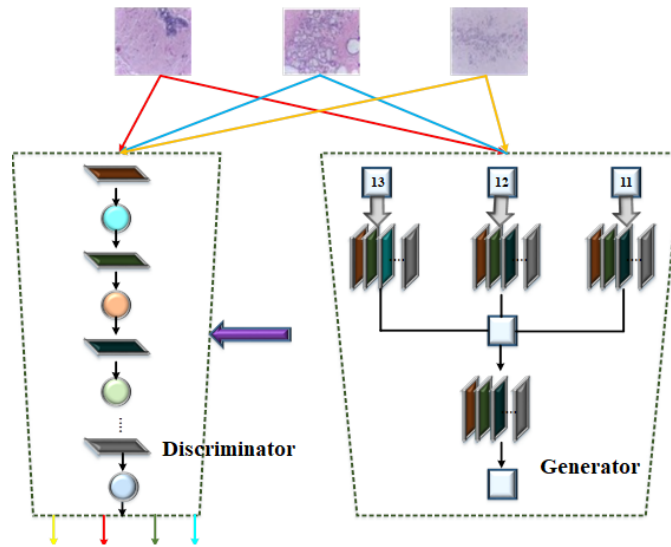


**Figure 2.** The proposed Generative Adversarial Network (GAN) for stain normalization refinement. The network learns an optimal stain distribution from a diverse set of histopathology images, generating normalized images that improve consistency and minimize variations for subsequent analysis

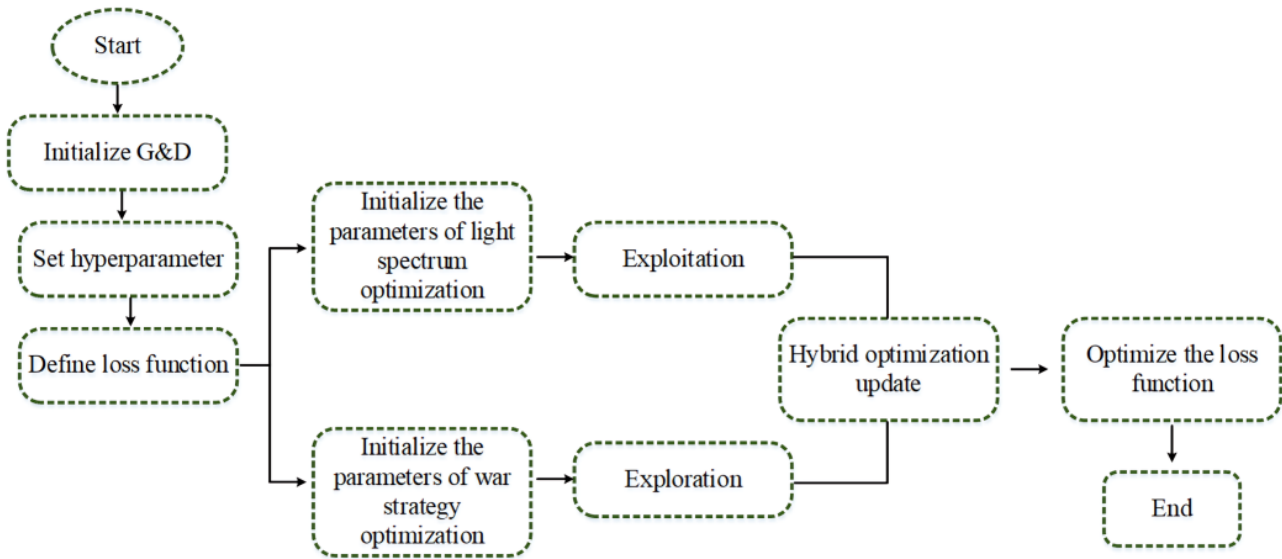


**Figure 3.** The proposed Hybrid Strategic Light Optimization (HSLO) algorithm, which combines the Light Spectrum Optimizer (LSO) and War Strategy Optimization (WSO) to minimize loss

Where,  $I(G(x))$  indicates the illumination (brightness) of the generated image, and  $I(T)$  is the illumination of the target image.

**Structural Preservation Loss** Structural Preservation Loss in the context of H and E-stained histopathology images refers to a loss function designed to maintain the key structural features of tissue samples during processes like stain normalization or enhancement . It ensures that important structural details, such as

cellular features and tissue morphology, are preserved despite changes in color or appearance.

$$LOSS_{Structural} = SSIM(G(x), T) \tag{4}$$

Where, SSIM means similarity measures in structure

$$Total\ loss = loss_{GAN} + \lambda_1 Loss_{color} + \lambda_2 Loss_{illum} + \lambda_3 Loss_{Structure} \tag{5}$$

### 3.4. Hybrid Strategic Light Optimization (HSLO)

To minimize the loss, Hybrid Strategic Light Optimization (HSLO) algorithm is used. It consists of Light Spectrum Optimizer (LSO) [26] and War Strategy Optimization (WSO) [27] shown in Figure 3. According to that, Hybrid Strategic Light Optimization (HSLO) algorithm can dynamically adjust the balance between G and D losses, preventing mode collapse and instability. It helps in selecting the best adversarial loss weight

$$\lambda_1, \lambda_2, \lambda_3 \quad (6)$$

maintain realism in stain-normalized images. The optimization process starts with the initialization of the GAN model parameters (Generator G, discriminator D) along with hyper parameters for both LSO and WSO. The loss functions include Reinhard stain normalization loss (color loss) to ensure color consistency, adversarial loss to guide the competition between G and D, and structural preservation loss to maintain nuclei morphology.

**LSO.** The Light Spectrum Optimizer (LSO) is a physically-inspired metaheuristic algorithm used to solve continuous optimization problems. The suggested algorithm is inspired by the way light disperses at different angles when it passes through raindrops, creating the beautiful rainbow spectrum that we see in the sky. The LSO search procedure starts with the random initialization of the initial population of white lights as follows:

$$\vec{a}^0 = l_{\text{bound}} + \text{RanV}_1 (u_{\text{bound}} - l_{\text{bound}}) \quad (7)$$

Where,  $\vec{a}^0$  is the initial solution,  $\text{V}_1$  denotes a vector of uniform values,  $u_{\text{bound}}$  and  $l_{\text{bound}}$  indicate the upper and lower bounds of the search space.

$$GI = \alpha \times r^{-1} \times P^{-1}(\alpha, 1) \quad (8)$$

This inversion generates a value greater than 1, allowing the search process to reach distant regions in the search space, thereby increasing the likelihood of finding better solutions.  $P^{-1}$  is used to compute this inversion for a given parameter value of  $\alpha$ .

$$A = \text{RandV}_2 \left( 1 - \left( \frac{t}{T_{\text{max}}} \right) \right) \quad (9)$$

Where,  $T_{\text{max}}$  denotes the maximum number of function evaluations. This indicates the lower and upper bounds of the search space based on probability between 0 and 1, called  $p$ . In particular, if the value of  $p$  is lower than a number generated randomly between 0 and 1, then the new candidate solution will be calculated as:

This inverse incomplete gamma function produces high numerical values from almost 0.8 to almost 5.5

for input amounts greater than 0.5. A highly generated value may push updated solutions outside the search boundary, and boundary checking can reintroduce infeasible solutions, causing randomization. To prevent this, (10) represents a factor that causes incomplete inverse gamma values, reducing its magnitude and avoiding excessive randomness. As iterations progress, both the inverse function and factor decrease, shifting optimization from exploration to exploitation, potentially leading to local minima. To support exploration, the inverse function and factor gamma are defined as the inverse of a random number between 0 and 1.

---

#### Algorithm 2 Hybrid Spectrum Light Optimizer (HSLO)

---

**Require:** Objective function *objective\_function*, bounds *bounds*, population size *population\_size*

**Require:** LSO iterations *lso\_iterations*, WSO iterations *wso\_iterations*

**Require:** Hyperparameters:  $\lambda_{\text{LSO}}$ ,  $\alpha_{\text{WSO}}$ ,  $\beta_{\text{WSO}}$ , number of cycles *cycles*

**Ensure:** Best solution *best\_solution*

```

1: Initialize best_solution = None
2: Initialize best_loss =  $\infty$ 
3: for each cycle in cycles do
4:   // Exploration Phase with LSO
5:   candidate_solution =
     light_spectrum_optimizer(obj_function, bounds,
     population_size, lso_iterations,  $\lambda_{\text{LSO}}$ )
6:   // Exploitation Phase with WSO
7:   refined_solution =
     war_strategy_optimizer(obj_fun, candidate_solu,
      $\alpha_{\text{WSO}}$ ,  $\beta_{\text{WSO}}$ , wso_iterations)
8:   // Evaluate the refined solution
9:   refined_loss = obj_fun(refined_solu)
10:  if refined_loss < best_loss then
11:    best_solution = refined_solution
12:    best_loss = refined_loss
13:  end if
14: end for
15: Return best_solution

```

---

**WSO** An algorithm for metaheuristic optimization that is based on ancient military strategy. War Strategy Optimization (WSO) is based on the strategic movement of army soldiers during the fight. War strategy is portrayed as an optimization process in which each soldier moves dynamically toward the optimal value. Set the soldier size, the dimensions of the war space (the dimensions of the problem), and the lower and higher bounds of the search space. The positions of the King (R), Army Commander (AC) and Soldier Size (P)

$$A_i(t+1) = A_i(t) + 2 \times \rho \times (AC - R) + \text{rand} \times (WE_i \times R - A_i - (t)) \quad (10)$$

Were,  $A_i(t+1)$  denotes the new position,  $A_i$  indicates the previous Army Commander position,  $R$  is the position of King,  $WE$  denotes weights. Search agent positions are updated based on the King, Commander, and army ranks. Soldier ranks reflect proximity to the fitness value. If the new position's fitness new is lower than the previous fitness the soldier adopts the new position.

$$A_i(t+1) = A_i(t) + \mathbf{1}_{(F_{\text{new}} \geq F_{\text{previous}})} + A_i(t) \times \mathbf{1}_{(F_{\text{new}} < F_{\text{previous}})} \quad (11)$$

If the soldier updates the position successfully, the rank  $Rank_i$  of the soldier will be upgraded.

$$Rank_i = (Rank_i + 1) \cdot \mathbf{1}_{\{F_{\text{new}} \geq F_{\text{previous}}\}} + Rank_i \cdot \mathbf{1}_{\{F_{\text{new}} < F_{\text{previous}}\}} \quad (12)$$

Based on rank, new weight is calculated as,

$$WE_i = WE_i \times \left(1 - \frac{rank_i}{Max - iter}\right)^a \quad (13)$$

The second strategy update focuses on the King, army leader, and random troop positions. Meanwhile, ranking and weight updates remain unchanged .

$$A_i(t+1) = A_i(t) + 2 \times \rho \times (R - A_{\text{rand}}(t)) + \text{rand} \times WE_i \times ac - A_i(t) \quad (14)$$

In each iteration, identify the underperforming soldiers exhibiting the lowest fitness levels. We have evaluated many replacement methodologies. One straightforward approach is to substitute the weak soldier with a random soldier as specified.

$$AW_i(t+1) = Lboud + \text{rand} \times (Uband - Lband) \quad (15)$$

The alternative strategy involves repositioning the vulnerable soldier nearer to the median of the entire army during combat. This method enhances the algorithm's convergence characteristics .

$$AW_i(t+1) = -\left(1 - \text{randn} \cdot AW_i(t) - \text{mean}(A)\right) + R \quad (16)$$

$L$  denotes the luminance of the image.

**The Pearson Correlation Coefficient (PCC)** It is a statistical measure that quantifies the linear relationship or correlation between two variables or datasets. In the context of image processing, it measures the degree of similarity between the original and processed (eg. normalized) images, specifically indicating how strongly the intensity values of corresponding pixels in the two images are linearly related.

$$r = \frac{\sum_{i=1}^N (X_i - X)(Y_i - Y)}{\sqrt{\sum_{i=1}^N (X_i - X)^2 \sum_{i=1}^N (Y_i - Y)^2}} \quad (17)$$

**Iterative Process:** Alternate between the exploration phase (LSO) and the exploitation phase (WSO). This combination ensures that the model not only searches the parameter space effectively but also fine-tunes the solutions to converge on an optimal point. First, a round of exploration is performed to discover new solutions. Then, exploitation will be performed to refine and optimize those solutions. Iteration: Cycle 1: Explore with LSO to search the parameter space.

Cycle 2: Exploit with WSO to fine-tune the generator and discriminator weights. Repeat for multiple cycles until convergence or improvement plateaus. Objective function The hybrid optimization mechanism (exploration + exploitation) is governed by the following total loss function, ensuring both structural preservation and adversarial balance. During exploration (LSO), the goal is to discover new regions in the parameter space, and during exploitation (WSO), the focus shifts to fine-tuning these solutions.

**Algorithm 3** Training GAN with Hybrid Optimization

```

1: Initialize Generator (G) and Discriminator (D)
   networks
2: Set hyperparameters:
    $\lambda_{LSO}, \alpha_{WSO}, \beta_{WSO}, \lambda_{adv}, \lambda_{struct}$ 
3: Define loss functions:  $L_{adv}, L_{color}, L_{struct}$ 
4: for epoch = 1 to total_epochs do
5:   for each batch in data_loader do
6:     Train Discriminator (D)
7:      $D.zero\_grad()$ 
8:      $d\_loss\_real = L_{adv}(D(target\_images), 1)$ 
9:      $fake\_images = G(real\_images)$ 
10:     $d\_loss\_fake = L_{adv}(D(fake\_images.detach()), 0)$ 
11:     $d\_loss = d\_loss\_real + d\_loss\_fake$ 
12:     $d\_loss.backward()$ 
13:    Update D's parameters
14:    Train Generator (G)
15:     $G.zero\_grad()$ 
16:     $g\_loss\_adv = L_{adv}(D(fake\_images), 1)$ 
17:     $g\_loss\_color = L_{color}(fake\_images, target\_images)$ 
18:     $g\_loss\_struct =$ 
    $L_{struct}(fake\_images, target\_images)$ 
19:     $g\_loss = g\_loss\_color + \lambda_{adv} \cdot g\_loss\_adv +$ 
    $\lambda_{struct} \cdot g\_loss\_struct$ 
20:     $g\_loss.backward()$ 
21:    Update G's parameters
22:    Hybrid Optimization Update
23:    Adjust learning rates for  $G\_optimizer$  and
    $D\_optimizer$ 
24:    if iteration % log_interval == 0 then
25:      Print (epoch, iteration,  $d\_loss$ ,  $g\_loss$ )
26:    end if
27:  end for
28: end for

```

## 4. Result and Discussion

In this section, the results of the proposed ReinhardGAN-HSLO method are compared to those of other existing color normalisation methods, including Stain Colour Adaptive Normalisation the Reinhard Algorithm, the Modified Reinhard Algorithm, the Conventional Reinhard Algorithm with fuzzy logic, and Reinhard GAN (without optimisation) based on metrics. All of the approaches listed above were implemented and simulated using MATLAB. For experimentation, test histopathology photos of colon cancer are collected from NCT-CRC-HE-100K. For experimentation, 100 photos are taken from each of the databases.

### 4.1. Metrics Analysis

The proposed model and existing approaches are compared with the following metrics to analyse the performance.

**Peak Signal-to-Noise Ratio (PSNR)** PSNR can be used to evaluate the quality of the color-stained image after normalization against the original stained image. Since stain normalization aims to standardize the colors in histopathology images (like H and E staining in cancer tissue), it helps in reducing the variations caused by different imaging conditions.

$$PSNR = 10 \cdot \log_{10} \left( \frac{R^2}{MSE} \right) \quad (18)$$

**MSE** Mean Squared Error (MSE) is a widely used metric to measure the quality of a model by evaluating the difference between predicted (or normalized) and true (target) values. In the context of image normalization, MSE quantifies the pixel-wise difference between the original and the normalized image.

$$MSE = \frac{1}{M \times N} \sum_{i=1}^M \sum_{j=1}^N I(i, j) - K(i, j)^2 \quad (19)$$

Where,  $I(i, j)$  indicates the original image.  $K(i, j)^2$  indicates normalized image Dimension of image M and N.

**SSIM** The Structural Similarity Index Measure (SSIM) is a metric used to assess the similarity between two images, taking into account luminance, contrast, and structure.

$$SSIM(I, K) = \left( \frac{(2uIuK + C1)(2sigmaIK + C2)}{\mu(I)^2 + \mu(K)^2 + C1 (\sigma(I)^2 + \sigma(K)^2 + C2)} \right) \quad (20)$$

$uIuK$  indicates mean value,  $sigma(I)^2 \sigma(K)^2$  denotes variance of image  $sigmaIK$  represents covariance between two images

**Absolute Mean Luminance Error** It is a metric used to evaluate the luminance (brightness) preservation in an image after processing, such as in stain image normalization.

$$AMLE = \frac{1}{M \times N} \sum_{i=1}^M \sum_{j=1}^N |L(i, j) - (L(K(i, j)))| \quad (21)$$

**The Pearson Correlation Coefficient (PCC)** It is a statistical measure that quantifies the linear relationship or correlation between two variables or datasets. In the context of image processing, it measures the degree of similarity between the original and processed (e.g., normalized) images, specifically indicating how strongly the intensity values of corresponding pixels in the two images are linearly related.

$$r = \frac{\sum_{i=1}^N (X_i - X)(Y_i - Y)}{\sqrt{\sum_{i=1}^N (X_i - X)^2 \sum_{i=1}^N (Y_i - Y)^2}} \quad (22)$$

$X_i, Y_i$  denotes intensity values of the corresponding pixel from the original and normalised image  $X, Y$  represent mean intensity values

**AMCE** AMCE calculates the mean of the absolute colour differences between each corresponding pixel in two images (the original image and the normalized or processed image). The smaller the AMCE, the closer the color distribution in the processed image is to the original.

$$AMCE = \frac{1}{M \times N} \sum_{i=1}^M \sum_{j=1}^N C(I(i, j) - C(K(i, j)^o)) \quad (23)$$

$C(I(i, j))$  denotes colour pixel values of the pixel at position.

#### 4.2. Comparison analysis of the proposed model

**Qualitative analysis** Figure 4 represents the visual results of several color normalization algorithms. The analysis includes comparing the target image with two source images, demonstrating the effectiveness of different color normalization techniques: Stain Colour Adaptive Normalization [28], the Reinhard Algorithm, the Modified Reinhard Algorithm, the Conventional Reinhard Algorithm with Fuzzy Logic, the Reinhard GAN, and the Proposed Model.

**Quantitative Analysis** In this section, we compare the performance of the proposed model with traditional color normalization methods. We evaluate the results based on several metrics, including PSNR, SSIM, MSE, AMLE, AMCE, and PCC.

Table 2 compares the performance of the proposed model with other methods. The results show that the proposed ReinhardGAN-HSLO method outperforms existing approaches in terms of all evaluation metrics. Table 2 presents visual comparisons of several color normalization techniques applied to histopathology images. The proposed model exhibits superior color consistency and structural preservation. The performance of various colour normalisation methods is compared based on quality metrics such as SSIM, PSNR, AMLE, AMCE, PCC, and MSE, which are shown in Table 2. The Proposed Model consistently outperforms all other methods across these metrics.

The Proposed Model (with HSLO optimization) outperforms all prior color normalization methods using SSIM and AMLE. It has the best SSIM of 0.99 (showing strong structural similarity preservation) and the lowest AMLE of 0.05 (indicating low luminance error). The Reinhard GAN (Without Optimisation) has a SSIM of 0.92 and a AMLE of 0.1, showing gains over typical normalisation methods but still not as good as the proposed method. The Modified Reinhard Algorithm is the best classic method, with a SSIM of 0.91 and a AMLE of 0.18, improving colour consistency and error reduction. The Reinhard Algorithm and Conventional Reinhard with Fuzzy Logic have somewhat lower structural similarity and bigger luminance errors, with SSIM values of 0.9 and

0.88 and AMLE values of 0.28 and 0.2, respectively. The Stain Colour Adaptive Normalisation method has the lowest SSIM of 0.85 and the highest AMLE of 0.35, exhibiting severe colour normalisation disparities. The Proposed Model is effective, since it minimizes color fluctuation and enhances structural preservation compared to previous methods shown in Figure 5.

The Proposed Model (with HSLO optimisation) beats all other colour normalisation approaches, achieving the lowest AMCE (0.03) and highest PCC (0.98). The Reinhard GAN (Without Optimisation) also performs well, with AMCE: 0.08 and PCC: 0.96, showing big gains in colour accuracy. The Modified Reinhard Algorithm is balanced (AMCE: 0.12, PCC: 0.95) compared to the Reinhard Algorithm (AMCE: 0.18, PCC: 0.94) and Conventional Reinhard with Fuzzy Logic (AMCE: 0.15, PCC: 0.92). The Stain Colour Adaptive Normalisation has the lowest performance (AMCE: 0.25, PCC: 0.92), showing more chromatic deviation. Overall, the Proposed Model greatly boosts colour normalisation accuracy, exceeding all benchmark methodologies shown in Figure 6. The Proposed Model (with HSLO optimization) achieves the highest PSNR (41 dB), ensuring superior image quality with minimal distortion, surpassing all existing methods shown in Figure 7. The Reinhard GAN (Without Optimization) follows with 34.5 dB, showing notable improvement over traditional approaches.

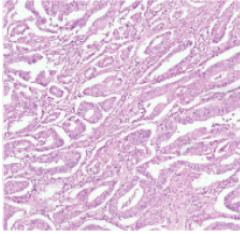
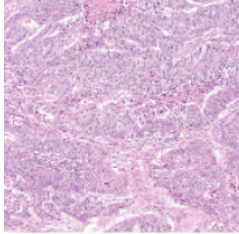
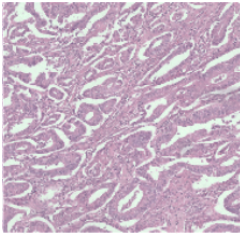
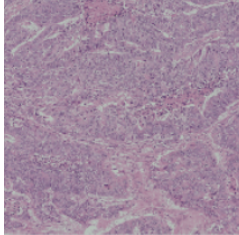
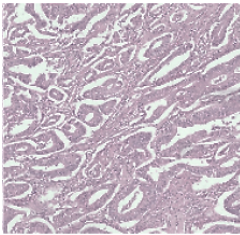
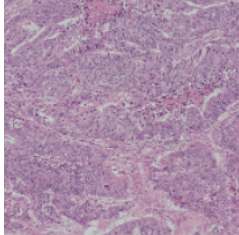
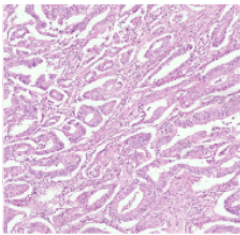
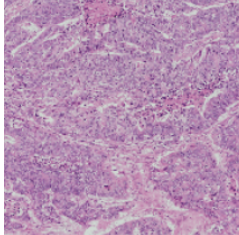
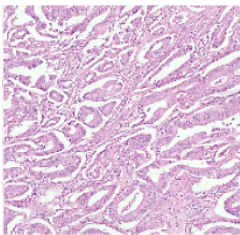
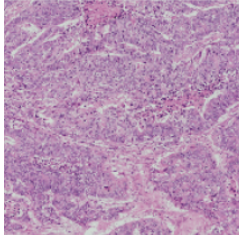
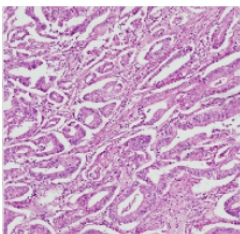
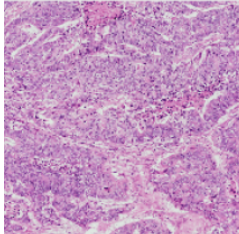
Among conventional techniques, the Modified Reinhard Algorithm (33.2 dB) performs best, outperforming the Reinhard Algorithm (32 dB) and Conventional Reinhard with Fuzzy Logic (31 dB). The Stain Colour Adaptive Normalization has the lowest PSNR (30.5 dB), indicating higher noise and distortion. The Proposed Model sets a new benchmark in color normalization by significantly enhancing image fidelity. The Proposed Model (with HSLO optimisation) has the lowest MSE (0.002), showing low reconstruction error and good colour constancy. The Reinhard GAN (Without Optimisation) follows with MSE: 0.005, a big improvement over traditional approaches shown in Figure 8.

Among traditional techniques, the Modified Reinhard Algorithm (0.008) outperforms the Reinhard Algorithm (0.01) and Conventional Reinhard with Fuzzy Logic (0.012). The Stain Colour Adaptive Normalisation has the highest MSE (0.015), meaning it deviates most from the reference photos. The Proposed Model sets a new standard in colour normalisation by minimising error and improving accuracy.

#### 4.3. Computational Analysis

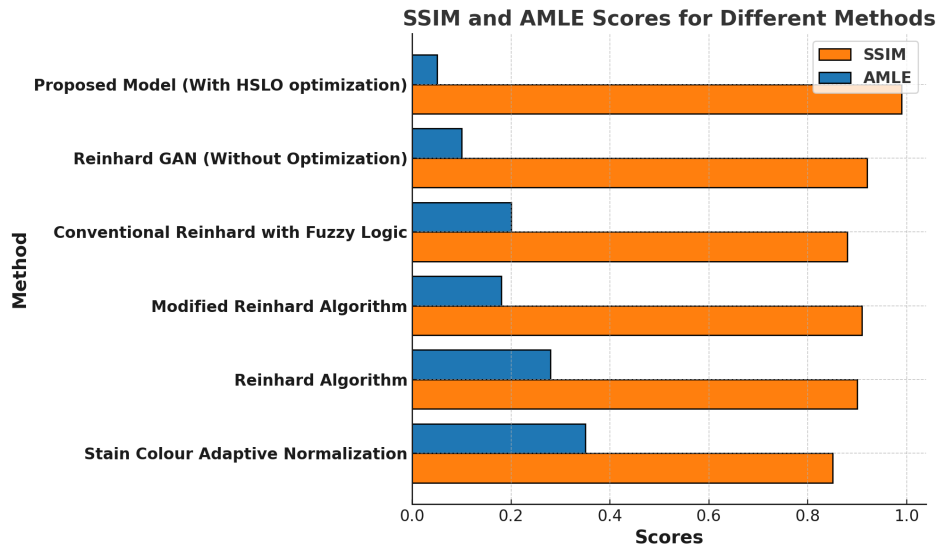
**Cost Analysis** In this section, cost and computational analysis are performed in Table 4. The cost comparison analysis is presented in Figure 9. Thus, the proposed model takes very little time compared to other

Table 2. Qualitative comparative analysis of different stain normalization methods

Method	Source Image 1	Source Image 2
Target Image		
Stain Colour Adaptive Normalization		
Reinhard		
Conventional Algorithm with Fuzzy Logic		
Reinhard GAN		
Proposed Reinhard GAN-HSLO		

**Table 3.** Quantitative comparison analysis of different stain normalization methods

Method	SSIM	PSNR	AMLE	AMCE	PCC	MSE
Stain Colour Adaptive Normalization	0.85	30.5	0.35	0.25	0.92	0.015
Reinhard Algorithm	0.90	32.0	0.28	0.18	0.94	0.010
Modified Reinhard Algorithm	0.91	33.2	0.18	0.12	0.95	0.008
Conventional Reinhard with Fuzzy Logic	0.88	31.0	0.20	0.15	0.92	0.012
Reinhard GAN (Without Optimization)	0.92	34.5	0.10	0.08	0.96	0.005
<b>Proposed Model (With optimization)</b>	<b>0.99</b>	<b>41.0</b>	<b>0.05</b>	<b>0.03</b>	<b>0.98</b>	<b>0.002</b>

**Figure 4.** Visual comparison of color normalization results across different algorithms. The target image and two source images are shown alongside outputs from Stain Colour Adaptive Normalization [28], the Reinhard Algorithm, the Modified Reinhard Algorithm, the Conventional Reinhard Algorithm with Fuzzy Logic, the Reinhard GAN, and the Proposed Model**Table 4.** Computing time and accuracy comparison for different methods

Method	Computing Time (s)	Accuracy (%)
Stain Colour Adaptive Normalization	7.23	88
Reinhard Algorithm	5.12	91
Modified Reinhard Algorithm	4.70	93
Conventional Reinhard with Fuzzy Logic	3.00	90
Reinhard GAN	2.50	95
<b>Proposed Reinhard GAN – HSLO</b>	<b>2.00</b>	<b>99</b>

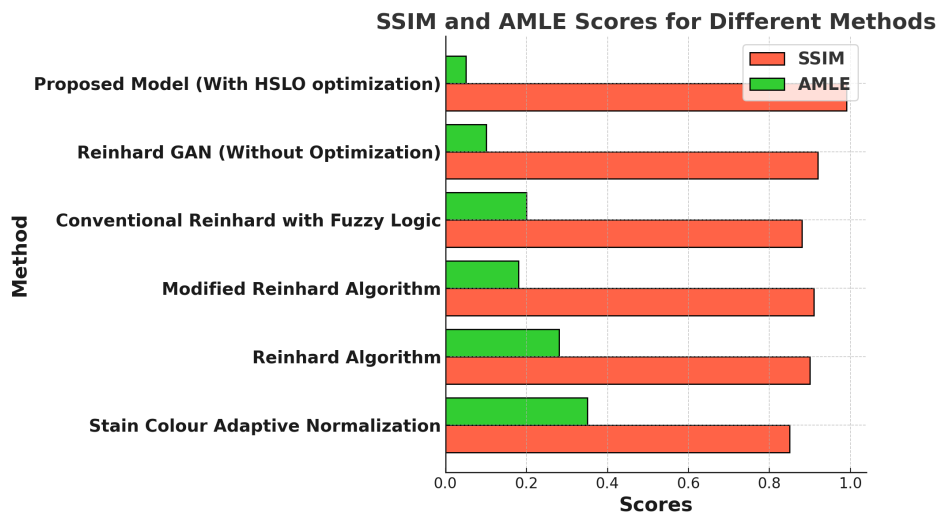


Figure 5. Comparative Analysis of structural Similarity Index Measure (SSIM) and Absolute Mean Color Error (AMCE) for different Stain Normalization Methods

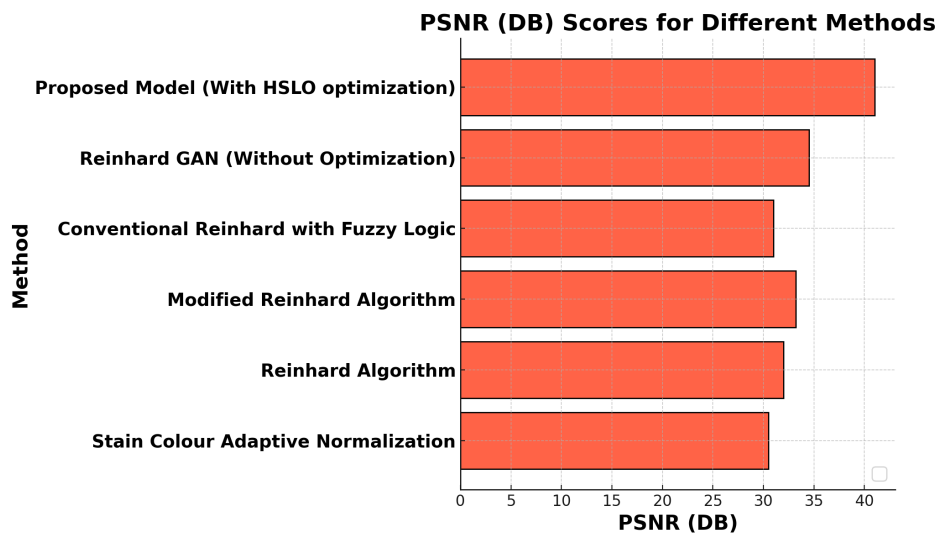


Figure 6. Comparative Analysis of Peak Signal to Noise Ratio (PSNR) for different Stain Normalization Methods

approaches and also appropriately reduces cost. The Proposed Model achieves the highest accuracy of 99%, with the shortest computing time of 2.0 seconds, making it the most efficient method in terms of both performance and speed. The GAN Combined with Reinhard Algorithm also performs well with 95% accuracy and a low computing time of 2.5 seconds. The Modified Reinhard Algorithm provides a good balance with 93% accuracy and 4.7 seconds of computing time, while the Reinhard Algorithm offers 91% accuracy in 5.12 seconds. The Conventional Reinhard with Fuzzy Logic method has an accuracy of 90% with a moderate computing time of 3.0 seconds, and the Stain Colour Adaptive Normalization method. However, it has the highest computing time of 7.23 seconds and achieves

a lower accuracy of 88%, making it the least efficient in comparison.

**Convergence Analysis** The Proposed Model demonstrates the fastest convergence, exhibiting a steep rise in accuracy throughout the epochs. The GAN Combined with Reinhard also shows a rapid increase in accuracy, though it lags slightly behind the proposed model in terms of convergence speed. In contrast, the Reinhard Algorithm and Modified Reinhard Algorithm display a more gradual improvement in accuracy over time. Finally, the Stain Colour Adaptive Normalization and Conventional Reinhard with Fuzzy Logic methods show the slowest rate of accuracy increase, indicating longer training times to reach optimal performance. The comparison analysis of convergence is shown in Figure 9.

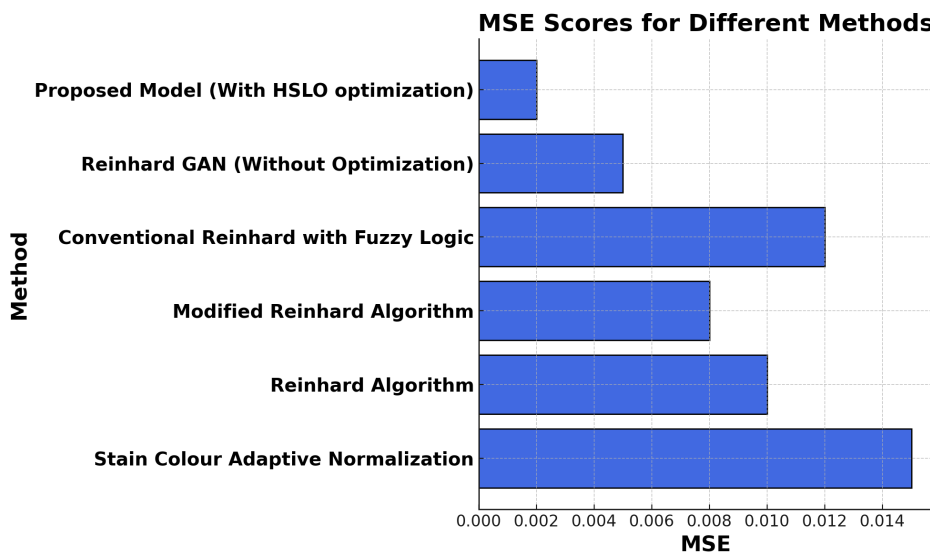


Figure 7. Comparative Analysis of Mean Square Error (MSE) for different Stain Normalization Methods

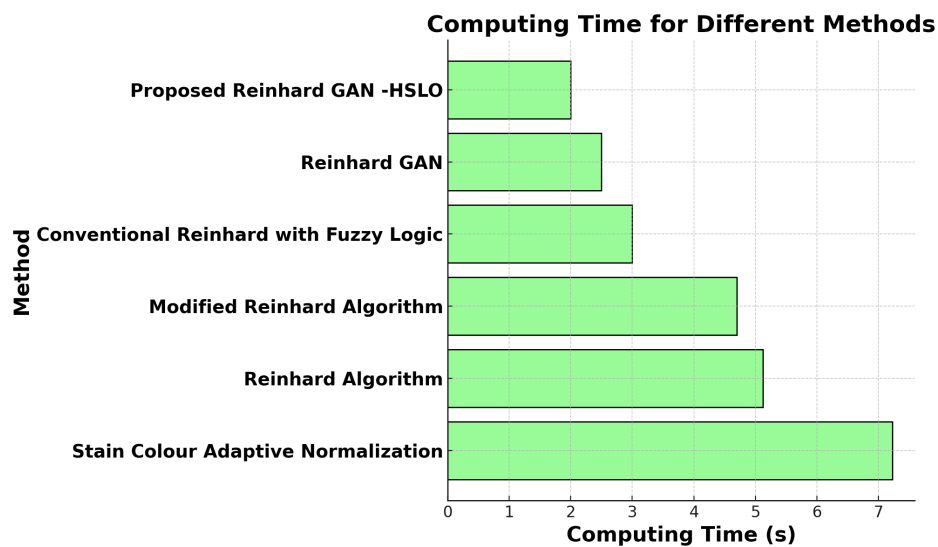
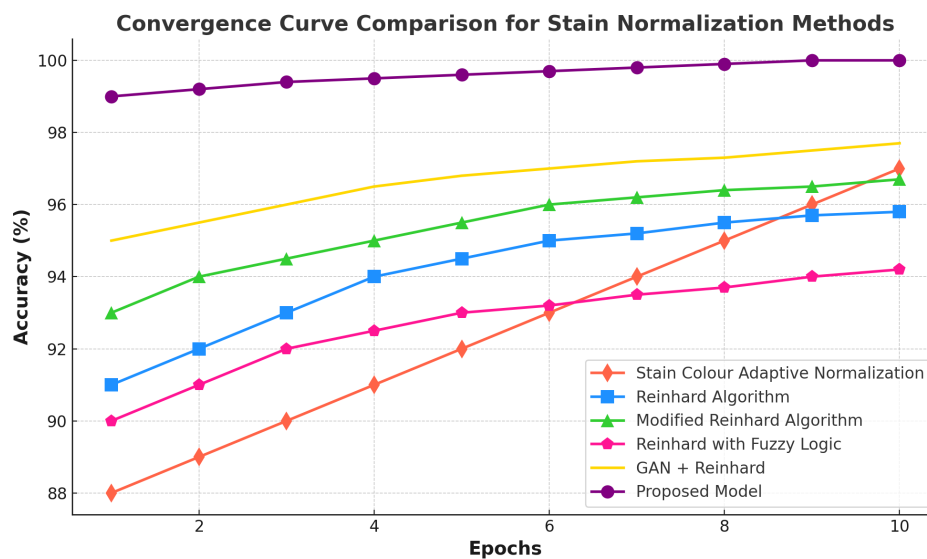


Figure 8. Cost Analysis for different Methods illustrating the computational based performance of Stain Normalization

## 5. Conclusion

Color normalization is a critical pre-processing technique for accurate interpretation of Haematoxylin and Eosin (H and E) stained colorectal cancer histopathology images. The proposed method, which integrates Reinhard normalization with a Generative Adversarial Network (ReinhardGAN) and utilizes a Hybrid Strategic Light Optimization (HSLO) algorithm, significantly enhances the consistency, contrast, and luminance of the images. This novel approach not only improves the color properties of H and E stained images but also reduces computational complexity and addresses inter-variability in background colors, making it more robust across diverse datasets. The experimental results show

that the proposed model outperforms traditional and benchmark techniques with Proposed Model shows the lowest AMLE (0.05), AMCE (0.03), and MSE (0.002), indicating minimal errors in color and structure. With the highest PCC (0.98), it demonstrates strong correlation with the target image. These results emphasize the model's superior ability to preserve color consistency and structural integrity, making it the most effective color normalization method. In addition, proposed model is outstanding perform in computational and loss analysis. Extending the model to handle multi-modal histopathology datasets (e.g., different cancer



**Figure 9.** Convergence analysis of different models, illustrating accuracy trends across epochs. The Proposed Model achieves the fastest convergence, followed by GAN combined with Reinhard, while Reinhard-based methods and fuzzy logic approaches show slower accuracy improvements over time

types or multi-site collections) would improve its generalizability. Finally, the integration of real-time processing capabilities for clinical applications, along with further exploration of the potential of unsupervised learning techniques, could be explored to make the model more adaptable in clinical workflows.

**Acknowledgements** The authors sincerely thank Manipal University Jaipur for providing a conducive research environment and the necessary infrastructure. The authors also acknowledge the high performance computing lab for facilitating this work through its computational resources and technical support.

## References

- [1] Obama YI, et al. Histopathological, cytological and radiological correlations in allergy and public health concerns: a comprehensive review. *J Asthma Allergy*. 2024;17:1333–1354.
- [2] Cong C. *Computer Vision in Histopathology Image Analysis: Preprocessing and Classification* [dissertation]. University of New South Wales; 2024. Available from: <http://hdl.handle.net/1959.4/102394>
- [3] Dibal NI, Garba SH, Jacks TW. Histological stains and their application in teaching and research. *Asian J Health Sci*. 2022;8(2):ID43.
- [4] Franchet C, et al. Bias reduction using combined stain normalization and augmentation for AI-based classification of histological images. *Comput Biol Med*. 2024;171:108130.
- [5] Martínez-Del-Río-Ortega R, et al. Brain tumor detection using magnetic resonance imaging and convolutional neural networks. *Big Data Cogn Comput*. 2024;8(9):123.
- [6] Uchikov P, et al. Artificial intelligence in the diagnosis of colorectal cancer: a literature review. *Diagnostics*. 2024;14(5):528.
- [7] Rehman ZU, et al. Comprehensive review on computational in-situ hybridization digital pathology using image analysis techniques: principles and applications.
- [8] Faizal, Abas FS, Cheah PL, Looi LM, Toh YF. Comprehensive review on computational in-situ hybridization digital pathology using image analysis techniques: principles and applications.
- [9] Reinhard E, Adhikhmin M, Gooch B, Shirley P. Colour transfer between images. *IEEE Comput Graph Appl*. 2001;21(5):34–41.
- [10] Guo Y, Shahin AI, Garg H. An indeterminacy fusion of encoder-decoder network based on neutrosophic set for white blood cells segmentation. *Expert Syst Appl*. 2024;246:123156.
- [11] Roy S, Panda S, Jangid M. Modified reinhard algorithm for color normalization of colorectal cancer histopathology images. In: *Proc 29th Eur Signal Process Conf (EUSIPCO)*; 2021. p. 1020–1024.
- [12] Piórkowski A, Gertych A. Color normalization approach to adjust nuclei segmentation in images of hematoxylin and eosin stained tissue. In: *International Conference on Information Technologies in Biomedicine*. Cham: Springer; 2018. p. 253–262.
- [13] Roy S, Lal S, Kini JR. Novel color normalization method for hematoxylin eosin stained histopathology images. *IEEE Access*. 2019;7:28982–28998.
- [14] Rabeya RA, et al. An experimental comparison and quantitative analysis on conventional stain normalization for histopathology images. 2024;27(11):1268–1288.
- [15] Yengce-Tasdemir SB, et al. Improved classification of colorectal polyps on histopathological images with ensemble learning and stain normalization. *Comput*

- Methods Programs Biomed. 2023;232:107441.
- [16] Lee J, et al. Unsupervised machine learning for identifying important visual features through bag-of-words using histopathology data from chronic kidney disease. *Sci Rep.* 2022;12(1).
- [17] Hetz MJ, Bucher TC, Brinker TJ. Multi-domain stain normalization for digital pathology: a cycle-consistent adversarial network for whole slide images. *Med Image Anal.* 2024;94:103149.
- [18] Alhassan AM. A generative adversarial network to Reinhard stain normalization for histopathology image analysis. *Ain Shams Eng J.* 2024;15(10):102955.
- [19] Rehman ZU, et al. Comprehensive analysis of color normalization methods for HER2-SISH histopathology images. *J Eng Sci Technol.* 2024;19:146–159.
- [20] Kausar T, et al. SA-GAN: stain acclimation generative adversarial network for histopathology image analysis. *Appl Sci.* 2021;12(1):288.
- [21] Hoque MZ, et al. Stain normalization methods for histopathology image analysis: a comprehensive review and experimental comparison. *Inf Fusion.* 2024;102:101997.
- [22] Moghadam AZ, et al. Stain transfer using generative adversarial networks and disentangled features. *Comput Biol Med.* 2022;142:105219.
- [23] Wagner SJ, et al. Structure-preserving multi-domain stain color augmentation using style-transfer with disentangled representations. In: *Int Conf Med Image Comput Comput Assist Interv.* Cham: Springer; 2021. p. 323–332.
- [24] Wong IHM, et al. Slide-free histological imaging by microscopy with ultraviolet surface excitation using speckle illumination. *Photonics Res.* 2021;10(1):120–125.
- [25] Nazki H, et al. MultiPathGAN: Structure preserving stain normalization using unsupervised multi-domain adversarial network with perception loss. In: *Proc 38th ACM/SIGAPP Symp Appl Comput*; 2023. p. 1450–1457.
- [26] Abdel-Basset M, et al. Light spectrum optimizer: A novel physics-inspired metaheuristic optimization algorithm. *Mathematics.* 2022;10(19):3466.
- [27] Ayyarao TSLV, et al. War strategy optimization algorithm: a new effective metaheuristic algorithm for global optimization. *IEEE Access.* 2022;10:25073–25105.
- [28] Cong C, et al. Colour adaptive generative networks for stain normalisation of histopathology images. *Med Image Anal.* 2022;82:102580.